

Submitted to the  
XXII International Symposium on Lepton-Photon Interactions at High  
Energy  
30 June - 5 July, Uppsala, Sweden

---

Abstract: 256

Sessions: EW&B, QCD/HS

# Observation of large rapidity gap events in charged and neutral current high $Q^2$ DIS at HERA

ZEUS Collaboration

28th June 2005

## Abstract

Events with a large rapidity gap have been observed in  $e^+p$  charged current (CC) deep inelastic scattering with the ZEUS detector at HERA using an integrated luminosity of  $65 \text{ pb}^{-1}$ . The diffractive CC cross section was measured in the kinematic range  $Q^2 > 100 \text{ GeV}^2$  and  $x_P < 0.05$ , where  $Q^2$  is the negative square of the four-momentum of the exchanged boson and  $x_P$  is the fraction of the incoming proton momentum carried by the diffractive exchange. The cross section is presented differentially in  $Q^2$ ,  $x_P$  and the longitudinal momentum fraction of the exchange that is carried by the struck quark,  $\beta$ . The ratio of diffractive to inclusive neutral current cross sections has been determined at  $Q^2 > 200 \text{ GeV}^2$ . This ratio is compared to that for the CC process measured in the same kinematic region.



# 1 Introduction

Diffractive processes are a significant component of the total neutral current (NC) deep inelastic scattering (DIS) cross section measured at HERA. Diffractive exchange leads to the formation of a large rapidity gap (LRG) in the hadronic final state, located between the exchanged boson and the proton fragmentation regions.

Along with diffractive NC processes, charged current (CC) induced diffraction is also of interest since it is a purely weak process unlike the NC which is dominated by photon exchange. LRG events in CC DIS,  $e^+p \rightarrow \bar{\nu}_e XY$ , have already been observed at HERA [1], where one event selected from 1994  $e^+p$  data in the ZEUS CC DIS sample was found with a LRG. With increased luminosity the ZEUS collaboration reported 9 events observed and measured a total cross section [2] for  $Q^2 > 200 \text{ GeV}^2$ . One possible interpretation of such events is a diffractive exchange between the virtual  $W$  boson and the proton.

The aim of this paper is to study diffraction in the electroweak regime by searching for events with a LRG in the CC DIS data taken in 1999 and 2000. The measurement has been performed for  $Q^2 > 100 \text{ GeV}^2$ . Lower background is expected in the LRG CC analysis compared to that in the inclusive analysis, which allows the kinematic region to be extended to lower values of  $Q^2$ . This results in improved statistical precision compared to the previous measurement and allows single-differential cross-section measurements. Comparing to NC diffractive DIS allows factorization to be tested in diffractive DIS at HERA. The analysis of the NC channel was performed for  $Q^2 > 200 \text{ GeV}^2$ . Because of the same analysis technique, many systematic effects cancel in this comparison.

## 2 Experimental setup

A detailed description of the ZEUS detector can be found elsewhere [3]. A brief outline of the components that are most relevant for this analysis is given below.

Charged particles are tracked in the central tracking detector (CTD) [4], which operates in a magnetic field of 1.43 T provided by a thin superconducting coil. The CTD consists of 72 cylindrical drift chamber layers, organized in 9 superlayers covering the polar-angle<sup>1</sup> region  $15^\circ < \theta < 164^\circ$ . The transverse-momentum resolution for full-length tracks is  $\sigma(p_T)/p_T = 0.0058p_T \oplus 0.0065 \oplus 0.0014/p_T$ , with  $p_T$  in GeV.

---

<sup>1</sup> The ZEUS coordinate system is a right-handed Cartesian system, with the  $Z$  axis pointing in the proton beam direction, referred to as the “forward direction”, and the  $X$  axis pointing left towards the center of HERA. The coordinate origin is at the nominal interaction point. The pseudorapidity is defined as  $\eta = -\ln(\tan \frac{\theta}{2})$ , where the polar angle,  $\theta$ , is measured with respect to the proton beam direction.

The high-resolution uranium–scintillator calorimeter (CAL) [5] consists of three parts: the forward (FCAL), the barrel (BCAL) and the rear (RCAL) calorimeters. Each part is subdivided transversely into towers and longitudinally into one electromagnetic section (EMC) and either one (in RCAL) or two (in BCAL and FCAL) hadronic sections (HAC). The smallest subdivision of the calorimeter is called a cell. The CAL energy resolutions, as measured under test-beam conditions, are  $\sigma(E)/E = 0.18/\sqrt{E}$  for electrons and  $\sigma(E)/E = 0.35/\sqrt{E}$  for hadrons ( $E$  in GeV).

In 1998-2000, the forward plug calorimeter (FPC) [6] was installed in the beam hole of the FCAL, with a small hole of radius 3.15 cm in the center to accommodate the beam pipe. The FPC increased the forward calorimeter coverage by about 1 unit of pseudo-rapidity to  $\eta < 5$ . The FPC was tested at CERN with electron and hadron beam. The energy resolution was  $\sigma(E)/E = 0.41/\sqrt{E} \oplus 0.062$  and  $\sigma(E)/E = 0.65/\sqrt{E} \oplus 0.06$  for electrons and pions, respectively, with  $E$  in GeV.

### 3 Monte Carlo simulation

Monte Carlo (MC) simulations were used to determine the selection efficiency, to estimate  $ep$  background rates and to extract cross sections.

Diffractive NC and CC events were modelled with the RAPGAP 2.08/06 [7] generator, in which colour singlet exchange occurs between virtual boson and proton.

Non-diffractive NC and CC events were produced with the DJANGO 1.1 [8] generator interfaced to the colour-dipole model of ARIADNE 4.10 [9] for the fragmentation. As a systematic check, the MEPS model of LEPTO 6.5 [10] was used. Both programs use the Lund string model of JETSET 7.4 [11–13] for the hadronisation.

As an alternative, the MEPS model of LEPTO including soft colour interaction (SCI) which give rise to large rapidity gap events without introducing the concept of diffractive exchange was used instead of the combination of the ARIADNE and RAPGAP samples.

Photoproduction background was estimated using events simulated with HERWIG 5.9 [14]. The background from di-lepton production was estimated using the GRAPE [15] generator, and the background from  $W$  production was generated with EPVEC [16] program. Diffractive photoproduction background was simulated using RAPGAP.

### 4 Data sample

The data sample corresponding to an integrated luminosity of  $65.1 \pm 1.5 \text{ pb}^{-1}$ , collected during the running periods of 1999 and 2000 when HERA collided 27.5 GeV positrons

with 920 GeV protons, yielding a centre-of-mass energy of  $\sqrt{s} = 318$  GeV.

The reconstruction of the kinematic variables of the CC DIS event candidates were described in detail in a previous publication [17]. The Bjorken scaling variables  $x_{\text{Bj}}$  and  $y$ , as well as  $Q^2$ , were reconstructed using the Jacquet-Blondel method [18]. This CC sample was selected using a similar selection to that of the inclusive CC measurement [17]. The special care for very forward events that escape the geometrical acceptance of the CTD is superfluous when selecting especially LRG event-topologies. The main criteria to select CC events are described below:

- a primary vertex position, determined from the CTD tracks, was required to be in the range  $|Z_{\text{VTX}}| < 50$  cm;
- missing transverse momentum, arising from the energetic final-state neutrino which escapes detection, calculated from CAL energy deposits was required to be greater than 8 GeV;
- at least one “good” track was required that is associated with the event vertex, has a transverse momentum exceeding 0.2 GeV and a polar angle in the range  $15^\circ$  to  $164^\circ$ ;
- the kinematic requirements  $Q^2 > 100 \text{ GeV}^2$ ,  $x_{\text{Bj}} < 0.05$  and  $y < 0.9$  were imposed.

After these requirements, 833 CC events remained.

The reconstruction and selection criteria for NC event candidates is identical to that of an inclusive NC measurement [19]. The kinematic region is  $Q^2 > 200 \text{ GeV}^2$ ,  $x_{\text{Bj}} < 0.05$  and  $y < 0.9$ . The main selection criteria was the identification of a scattered positron. The track associated with the positron was required to originate from the primary event vertex, which rejects most of non- $ep$  collision background. The kinematic variables were reconstructed using the double angle (DA) method [20]. In total 17680 NC events were selected.

## 5 Large rapidity gap selection

To establish the presence of events with a LRG, the variable  $\eta_{\text{max}}$ , defined as the pseudo-rapidity of the energy deposit in the CAL, above 400 MeV, closest to the proton direction was considered. The distribution for the NC candidates is shown in Fig. 1. An excess of events with a LRG over non-diffractive (ARIADNE) MC expectation is observed in the region of  $\eta_{\text{max}} < 3$ .

The following criteria were applied to both the NC and CC samples to select LRG events:

- $E_{\text{FPC}} < 1.0$  GeV, where  $E_{\text{FPC}}$  is the energy deposited in the FPC. This cut suppresses the contribution from non-diffractive interactions, as shown for the NC sample on the

bottom plot in Fig. 1. It limits the mass of the proton remnant,  $M_Y$ , to approximately 2.3 GeV;

- $\eta_{\max} < 2.9$ . This cut reduces the remaining non-diffractive background and ensures a gap of at least two units of rapidity between the hadronic system measured in the detector and the rest of the hadronic final state that escapes detection through the beam pipe in proton direction;
- $x_P < 0.05$ , where  $x_P = \frac{q \cdot (P - P')}{q \cdot P}$  is the fraction of proton four-momentum carried by the exchanged colour singlet (pomeron). The variables  $q$ ,  $P$  and  $P'$  denote the four-momenta of the virtual  $W^+$  boson, the initial and final proton, respectively. This cut rejects non-diffractive events.

In total 17 CC event candidates and 1929 NC event candidates were selected out of the previous selection samples by the LRG requirements.

The upper plots in Fig. 2 show the distributions of relevant variables for NC DIS events for data and the sum of non-diffractive (ARIADNE) and diffractive (RAPGAP) MC simulations. The MC simulations describe well both the inclusive NC sample and the LRG subsample. The bottom plots in Fig. 2 show the distribution of diffractive variables  $\log(x_P)$  and  $\beta$  for LRG NC DIS events after statistical subtraction of non-diffractive background, where  $\beta$  is the fraction of Pomeron momentum carried by the struck parton. The agreement with the prediction of the diffractive (RAPGAP) MC simulation is satisfactory.

Figure 3 shows the distributions of relevant variables for NC DIS events together with the results of the MEPS with SCI included MC simulation. The rate of events with a LRG expected by this MC model is smaller than observed in the data. In addition, the distribution of track multiplicity in inclusive sample is not described by this model, in contrast to the ARIADNE generator. The MEPS version without SCI describes the track multiplicity distribution better, but the rate of a LRG events is reduced (not shown). This corresponds to the result of the earlier CC measurement [2].

Figure 4 shows the distributions of relevant variables for LRG selected CC DIS events for data and the sum of non-diffractive (ARIADNE) and diffractive (RAPGAP) MC simulations. The diffractive component is well described by the simulation.

## 6 Results

The LRG cross section for CC,  $\sigma^{\text{LRG}}(e^+p \rightarrow \bar{\nu}XY)$ , and NC,  $\sigma^{\text{LRG}}(e^+p \rightarrow e^+XY)$ , was determined by correcting the excess of LRG events over the background estimation for detector acceptance using the diffractive MC, such that:

$$\sigma^{\text{LRG}} = (N - N_{\text{bkg}})/(A\mathcal{L}),$$

where  $N$  is the number of LRG events observed in the data,  $N_{\text{bkg}}$  is the number of background as expected from the ARIADNE simulation,  $A$  is the acceptance given by the diffractive (RAPGAP) MC simulation and  $\mathcal{L}$  is the integrated luminosity.

The overall systematic uncertainty in the cross section and ratio of cross sections was obtained by summing in quadrature the uncertainties listed below:

- selection of large rapidity gap events. Systematic checks were performed by varying the cuts on  $\eta_{\text{max}}$  by  $\pm 0.1$  and on  $E_{\text{FPC}}$  by  $\pm 0.5$  GeV. This resulted in changes of less than  $\pm 20\%$  in both diffractive cross section and in ratio of cross sections;
- parton-shower scheme [17]. The MEPS simulation without SCI was used instead of the ARIADNE model for simulation of non-diffractive events. This lead to changes in the diffractive cross sections of usually less than  $\pm 5\%$ , but up to  $8\%$  in individual bins, and less than  $\pm 10\%$  in the ratio of cross sections;
- uncertainty of the calorimeter energy scale [17]. This uncertainty was  $\pm 3\%$  in the cross sections and assumed to cancel in the ratio of cross sections;
- uncertainty in the non-diffractive background subtraction. This uncertainty was found to be  $\pm 50\%$ . The effect on both diffractive cross sections and cross sections ratio was  $\pm 15\%$ , but increasing to  $\pm 30\%$  in individual bins;

The ratio of LRG cross section to the total cross section was measured in the kinematic region of  $Q^2 > 200$  GeV<sup>2</sup> and  $x_{\text{Bj}} < 0.05$  for both NC and CC processes. These ratios were found to be compatible as shown on Fig. 5. The CC LRG differential cross section  $d\sigma/dQ^2$ ,  $d\sigma/dx_{\mathcal{P}}$  and  $d\sigma/d\beta$  were measured on the extended kinematic region of  $Q^2 > 100$  GeV<sup>2</sup> and are shown in Fig. 6. The shapes of the cross sections are well described by the RAPGAP prediction. The absolute prediction is lower but consistent with the data.

## 7 Conclusions

The analysis of LRG events in the kinematic region  $x_{\mathcal{P}} < 0.05$  and  $Q^2 > 100(200)$  GeV<sup>2</sup> in the CC(NC) DIS has been presented. The results have been compared with predictions of the diffractive RAPGAP and MEPS, with SCI included MC simulations.

The rate of LRG events in CC and NC DIS processes and its  $Q^2$ ,  $x_{\mathcal{P}}$  and  $\beta$  dependencies are well described by the RAPGAP predictions, while SCI model expectation is significantly smaller than observed in the data for NC process. A similar indication, however with lower statistical precision, was reported previously for CC process at  $Q^2 > 200$  GeV<sup>2</sup>. These observations indicate that formation of LRG events both in NC and CC DIS is due to the exchange of the colour singlet state between the proton and the photon or  $W$  boson.

The ratio of CC LRG cross section to the total CC cross section was found to be compatible with the corresponding measurement for the NC process. This result suggests that the probability of diffractive excitation of the photon is similar to that of the  $W$  boson.

## References

- [1] ZEUS Coll., M. Derrick et al., *Z. Phys.* **C 72**, 47 (1996).
- [2] ZEUS Coll., *Observation of Large Rapidity Gap Events in Charged Current High  $Q^2$  DIS at HERA*. Abstract 229, International Conference on High Energy Physics, Beijing, China, 2004.
- [3] ZEUS Coll., U. Holm (ed.), *The ZEUS Detector*. Status Report (unpublished), DESY (1993), available on <http://www-zeus.desy.de/bluebook/bluebook.html>.
- [4] N. Harnew et al., *Nucl. Inst. Meth.* **A 279**, 290 (1989);  
B. Foster et al., *Nucl. Phys. Proc. Suppl.* **B 32**, 181 (1993);  
B. Foster et al., *Nucl. Inst. Meth.* **A 338**, 254 (1994).
- [5] M. Derrick et al., *Nucl. Inst. Meth.* **A 309**, 77 (1991);  
A. Andresen et al., *Nucl. Inst. Meth.* **A 309**, 101 (1991);  
A. Caldwell et al., *Nucl. Inst. Meth.* **A 321**, 356 (1992);  
A. Bernstein et al., *Nucl. Inst. Meth.* **A 336**, 23 (1993).
- [6] ZEUS Coll., FPC group, A. Bamberger et al., *Nucl. Inst. Meth.* **A 450**, 235 (2000).
- [7] H. Jung, *Comp. Phys. Comm.* **86**, 147 (1995).
- [8] H. Spiesberger, *HERACLES and DJANGO: Event Generation for ep Interactions at HERA Including Radiative Processes*, 1998, available on <http://www.desy.de/~hspiesb/djangoh.html>.
- [9] L. Lönnblad, *Comp. Phys. Comm.* **71**, 15 (1992).
- [10] G. Ingelman, A. Edin and J. Rathsman, *Comp. Phys. Comm.* **101**, 108 (1997).
- [11] T. Sjöstrand, *Comp. Phys. Comm.* **39**, 347 (1986).
- [12] T. Sjöstrand and M. Bengtsson, *Comp. Phys. Comm.* **43**, 367 (1987).
- [13] E. Norrbin and T. Sjostrand, *Eur. Phys. J.* **C 17**, 137 (2000).
- [14] G. Marchesini et al., *Comp. Phys. Comm.* **67**, 465 (1992).
- [15] T. Abe, *Comp. Phys. Comm.* **136**, 126 (2001).
- [16] U. Baur, J.A.M. Vermaseren and D. Zeppenfeld, *Nucl. Phys.* **B 375**, 3 (1992).
- [17] ZEUS Coll., S. Chekanov et al., *Eur. Phys. J.* **C 32**, 1 (2003).
- [18] F. Jacquet and A. Blondel, *Proceedings of the Study for an ep Facility for Europe*, U. Amaldi (ed.), p. 391. Hamburg, Germany (1979). Also in preprint DESY 79/48.
- [19] ZEUS Coll.; S. Chekanov et al., *Phys. Rev.* **D 70** (2004).

- [20] S. Bentvelsen, J. Engelen and P. Kooijman, *Proc. Workshop on Physics at HERA*, W. Buchmüller and G. Ingelman (eds.), Vol. 1, p. 23. Hamburg, Germany, DESY (1992);  
K.C. Höger, *Proc. Workshop on Physics at HERA*, W. Buchmüller and G. Ingelman (eds.), Vol. 1, p. 43. Hamburg, Germany, DESY (1992).

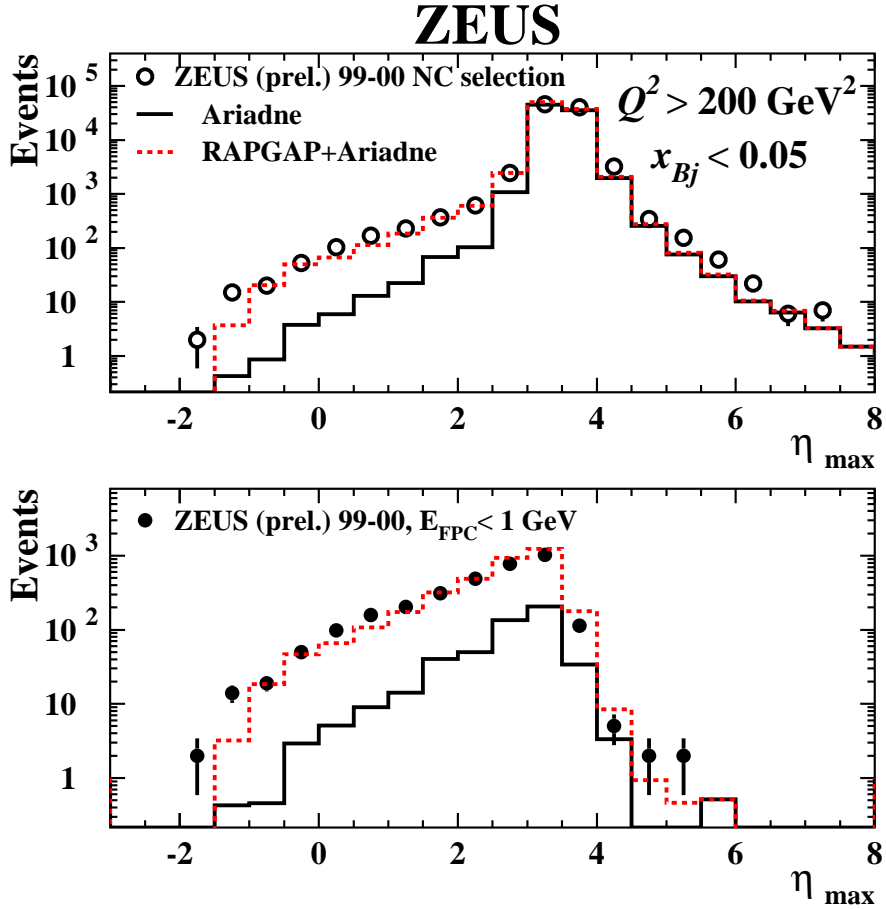


**Figure 1:** The distribution of  $\eta_{\max}$  is shown in the upper plot for NC DIS events in the kinematic range  $Q^2 > 200 \text{ GeV}^2$ ,  $y < 0.9$  and  $x_{Bj} < 0.05$ . The circles are the data points, the solid histogram is the result of the non-diffractive (ARIADNE) MC simulation and the dashed histogram is that of the sum of non-diffractive and diffractive (RAPGAP) MC sample. The bottom plot shows the same distributions with an additional requirement of  $E_{\text{FPC}} < 1 \text{ GeV}$ .

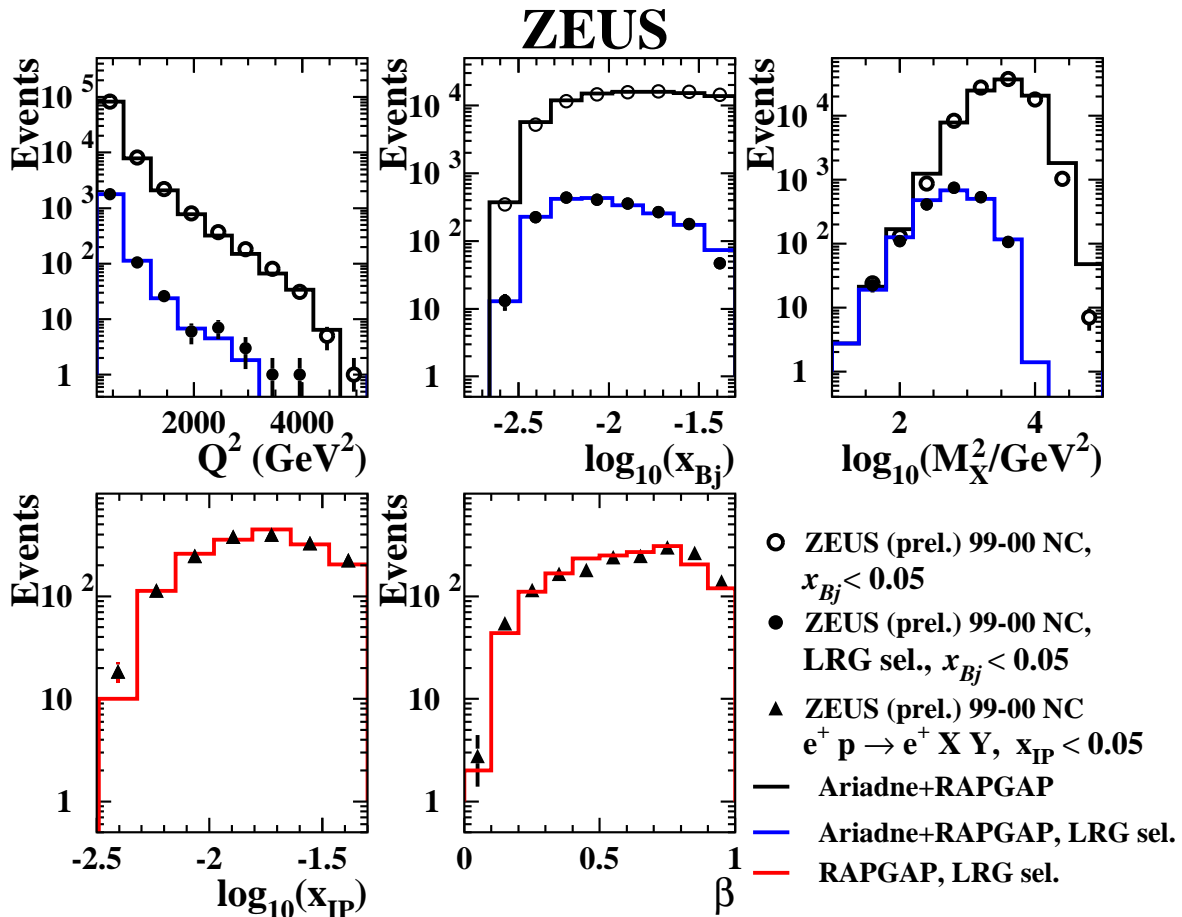


**Figure 2:** The upper plots show the distributions of  $Q^2$ ,  $\log x_{Bj}$  and  $\log M_X^2$ , where  $M_X$  is the mass of the hadronic system  $X$  measured in the CAL, for NC DIS events in the kinematic range of  $Q^2 > 200 \text{ GeV}^2$ ,  $y < 0.9$  and  $x_{Bj} < 0.05$ . The circles are the data points and the solid histograms are the sum of results of non-diffractive (ARIADNE) and diffractive (RAPGAP) MC simulations. The lower data points and MC histograms on each plot correspond to the subsamples satisfying the LRG selection criteria (see text). The bottom plots show the  $\log x_{IP}$  and  $\beta$  distributions of the NC DIS events satisfying the LRG selection criteria. The triangles are the data points after statistical subtraction of non-diffractive (ARIADNE) contribution. The solid histogram is the result of diffractive (RAPGAP) MC simulation.

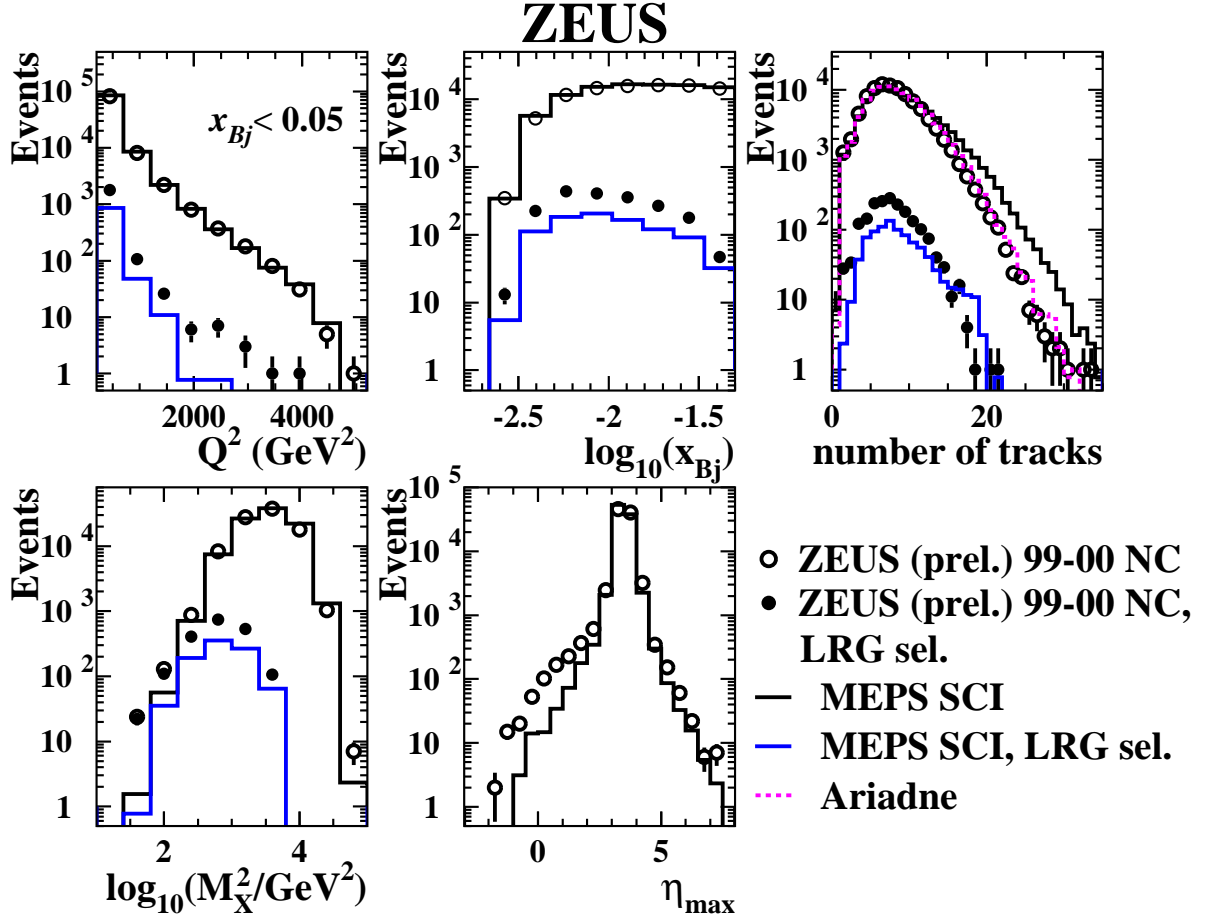


**Figure 3:** The distributions of  $Q^2$ ,  $\log x_{Bj}$ , number of “good” tracks,  $\log M_X^2$  and  $\eta_{\max}$  for NC DIS events in the kinematic range  $Q^2 > 200 \text{ GeV}^2$ ,  $y < 0.9$  and  $x_{Bj} < 0.05$ . The circles are the data points and the solid histograms are the results of MEPS with SCI included MC simulations. The dashed histogram superimposed on the distribution of the number of “good” tracks is the result of ARIADNE simulation. The lower data points and MC histograms on each plot correspond to the subsamples satisfying the LRG selection criteria (see text).

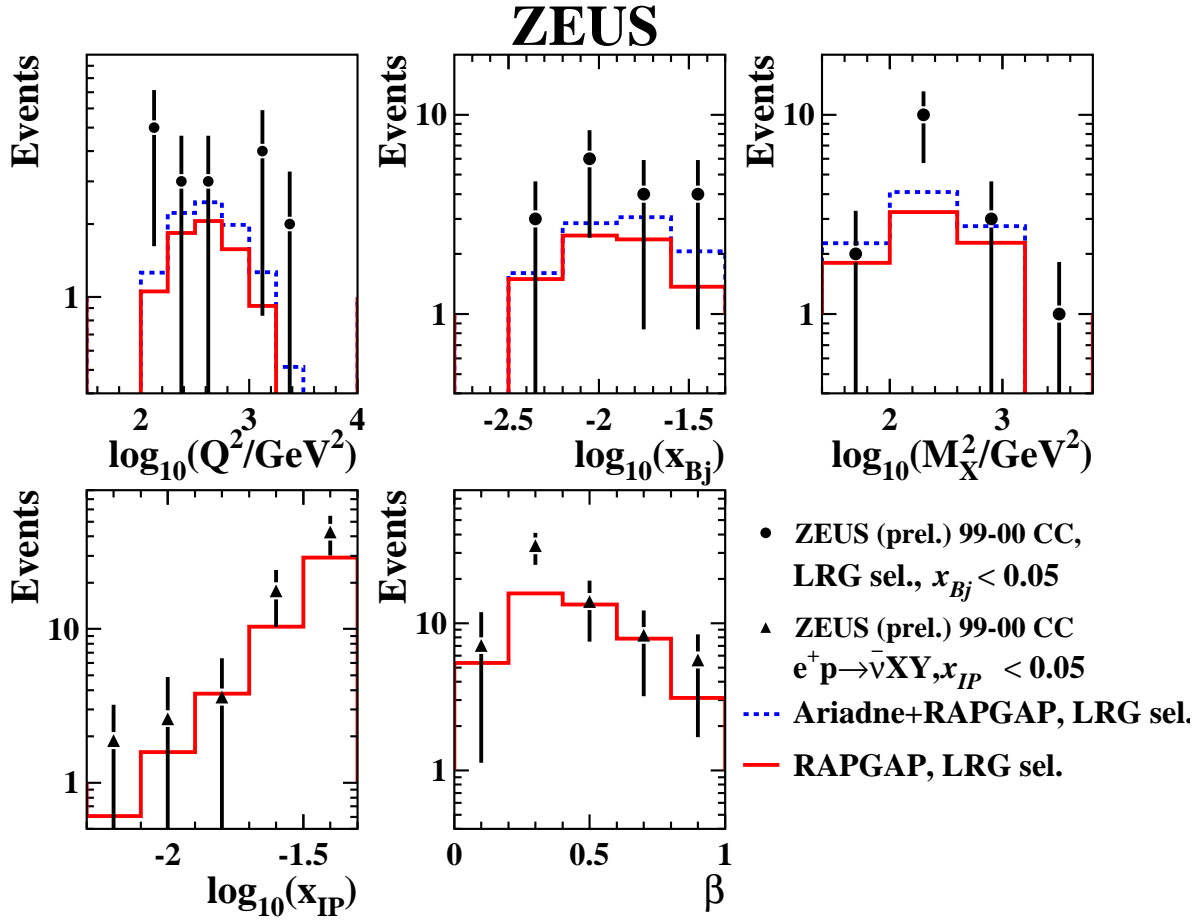


**Figure 4:** The distributions of  $\log Q^2$ ,  $\log x_{Bj}$  and  $\log M_X^2$  for LRG selected CC DIS events in the kinematic range  $Q^2 > 100 \text{ GeV}^2$ ,  $y < 0.9$  and  $x_{Bj} < 0.05$ . The circles are the data points and the dashed histograms are the sum of results of diffractive (RAPGAP), non-diffractive (ARIADNE) and other background MC simulations. The bottom plots show the  $\log x_P$  and  $\beta$  distributions of the CC DIS events satisfying the LRG selection criteria. The triangles are the data points after statistical subtraction of background contributions. The solid histogram is the result of diffractive (RAPGAP) MC simulation.

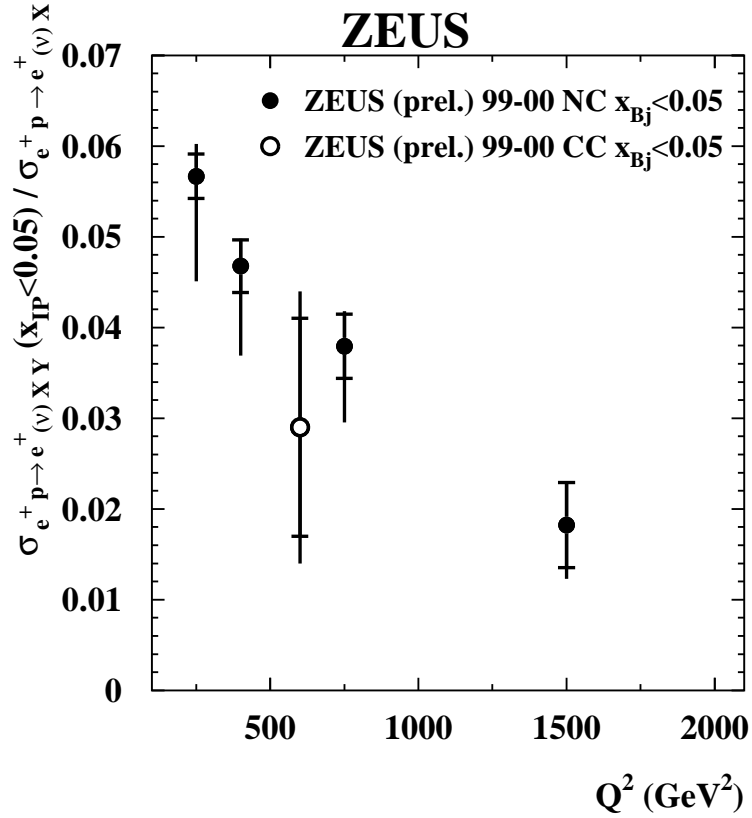


**Figure 5:** The ratio of the NC LRG cross section  $\sigma^{\text{LRG}}(e^+p \rightarrow e^+XY)$  in the kinematic region  $x_{\mathcal{P}} < 0.05$  to the total NC cross section  $\sigma^{\text{tot}}(e^+p \rightarrow e^+X)$  measured in the kinematic region  $x_{Bj} < 0.05$  as a function of  $Q^2$  is compared to the corresponding ratio for CC from a previous result.

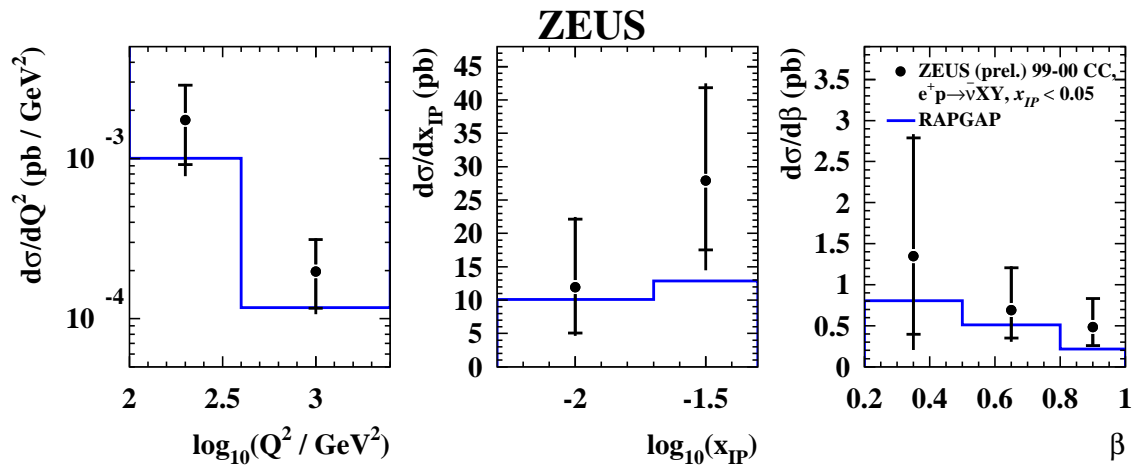


**Figure 6:** The CC LRG differential cross sections  $d\sigma/dQ^2$ ,  $d\sigma/dx_{\text{IP}}$  and  $d\sigma/d\beta$  measured for  $Q^2 > 100 \text{ GeV}^2$  and  $x_{\text{IP}} < 0.05$ . The measured values are compared to the RAPGAP prediction.